Scientia Iranica A (2021) 28(1), 124–137

SCIENTIA IRANICA

Sharif University of Technology
Scientia Iranica
Transactions A: Civil Engineering
http://scientiairanica.sharif.edu

Comparison of static pushover analysis and IDA-based probabilistic methods for assessing the seismic performance factors of diagrid structures

A. Seyedkazemi[a] and F. Rahimzadeh Rofooei[b,*]

a. *Department of Civil Engineering, Sharif University of Technology, Kish International Branch, Kish Island, Iran.*
b. *Department of Civil Engineering, Sharif University of Technology, Tehran, Iran.*

Received 14 September 2018; received in revised form 11 January 2019; accepted 26 August 2019

KEYWORDS
Diagrids;
Steel structures;
Pushover analysis;
Nonlinear dynamic analysis;
Seismic performance factors.

Abstract. The present study aims to reliably quantify the seismic response parameters of steel diagrid structural systems. To this end, in addition to the conventional Static Pushover Analysis (SPA), Dynamic Pushover Analysis (DPA) based on Incremental Dynamic Analysis (IDA) technique was taken into account. FEMA P-695 recommends a methodology for establishing Seismic Performance Factors (SPFs). The objective of the present study was to propose a simpler framework for estimating and validating SPFs while applying the concepts of FEMA P-695 guideline. The results showed that the R factors obtained through SPA procedure for steel diagrid systems were conservative and the IDA-based probabilistic method ensured a more rational value for the R coefficient. Furthermore, the proposed simplified method was in agreement with FEMA P-695 in predicting the collapse capacity of diagrid models.

1. Introduction

Today, diagrids are among the common structural systems utilized in high-rise buildings. These systems consist of diagonal grids on the perimeter of the buildings, making them stable even in the absence of columns [1]. Previous studies have focused on developing design criteria for diagrid structures in terms of stiffness and strength [2–4]. Other studies have investigated the ultimate capacity and performance of these structures under lateral loading [1,5,6]. The effect of the angle of the diagonal elements on the lateral load-carrying capability of diagrid structures was examined in References [7,8]. The results indicated that the diagrids had high stiffness and low ductility. Such characteristics facilitate the development of larger seismic loads than a tubular structure with the same properties.

Thus, it is essential to further study the seismic behavior of this structural system. Seismic Performance Factors (SPFs), i.e., the over-strength, ductility, and response modification factors (R), are appropriate indicators for describing the seismic behavior of structural systems. However, few studies have assessed the SPFs of diagrid systems; thus, they have not been explicitly introduced in the existing building codes. According to a study carried out by Baker et al. [9], the response modification factor was determined to be 3.64 for a particular diagrid structure using the Perform 3-D program [10]. In their study, the post-

*. *Corresponding author. Tel./Fax: +98 21 6616-4233*
E-mail addresses: seyedkazemi@kish.sharif.edu (A. Seyedkazemi); rofooei@sharif.edu (F. Rahimzadeh Rofooei)

doi: 10.24200/sci.2019.51555.2250

buckling behavior of diagonal members in compression was discarded. In addition, Static Pushover Analysis (SPA) was performed to calculate the initial R factor.

SPA was also employed to determine the SPFs of other structural systems [11–13] due to its simplicity and ease of use. However, the results obtained from SPA are strongly dependent on the employed lateral load pattern. To this end, many studies have been carried out in recent years to propose efficient load patterns for SPA [14–16]. However, the results obtained from the nonlinear dynamic analyses bear more similarity to the actual behavior of the structures than the SPA, especially in high-rise buildings. Nevertheless, there are still major concerns regarding the dependency of these responses on the frequency content of the selected earthquake records (i.e., the uncertainty in responses). Therefore, a reliable evaluation of the collapse capacity, seismic safety, and performance of structures is considered a major challenge in earthquake engineering [17].

Several studies have been carried out to compare the nonlinear static and dynamic analyses of some structural systems [18–21] and their results indicated that the damage patterns and failure mechanisms, drawn from the static and dynamic analyses, were not in agreement. In other words, these two methods could yield different results, particularly in the case of structures with severe damages. Therefore, both nonlinear static and dynamic analyses should be simultaneously utilized to accurately determine the seismic response parameters of the buildings.

The present study aims to present a new framework for a reliable evaluation of the SPFs and collapse assessment of steel diagrid systems. The proposed procedure, which is based on the concepts described in the FEMA P-695 [22], employs both SPA and Dynamic Pushover Analysis (DPA) to estimate the initial R-factor. In this research, nonlinear analyses were carried out using the OpenSees [23] program and the post-buckling behavior of diagonal members in compression was considered in their modeling.

2. Seismic Performance Factors (SPFs)

R factors are generally used in current building design codes to estimate the strength and deformation demands of seismic-force-resisting structural systems that are designed using linear methods while responding in a nonlinear range [22]. In order to calculate the SPFs, the structural capacity curve (base shear versus roof displacement curve) is replaced by a bilinear curve based on the equivalence in the energy absorption capacity as defined in ASCE 41-13 [24]. According to the idealized pushover curve in Figure 1, the seismic performance coefficients are defined as follows [25]:

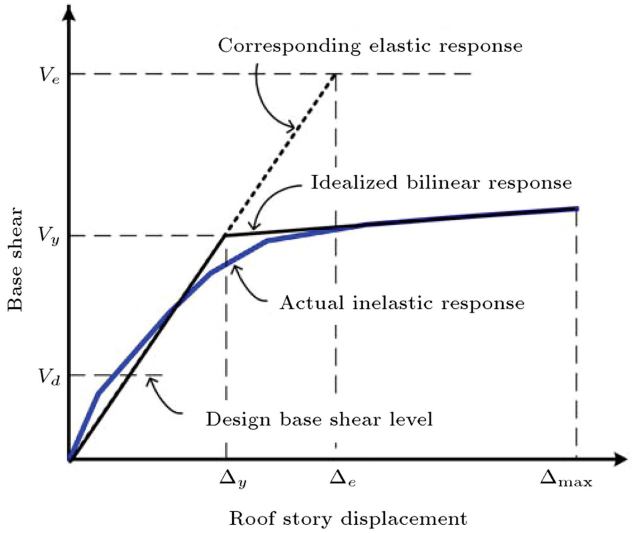

Figure 1. The lateral load-roof displacement relationship [25].

$$\mathrm{R} = \Omega_0 \; R_\mu R_r, \qquad \Omega_0 = \frac{V_y}{V_d},$$

$$R_\mu = \frac{V_e}{\mathrm{V_y}}, \qquad \mu = \frac{\Delta_{\max}}{\Delta_y}, \tag{1}$$

where R is the response modification factor, and V_y, V_d, and V_e represent the yield strength, design shear force, and elastic shear strength of the structure, respectively. The parameter Ω_0 represents the over-strength factor, R_μ is the ductility-related reduction factor, and R_r is the redundancy factor that is assumed 1.0 for diagrid structures due to their multiple bays in each direction to resist the lateral loadings. μ is the ductility factor of the system, $\Delta_{\max}$ is the roof displacement corresponding to the maximum base shear or target displacement, and Δ_y is the yield displacement of the system.

3. Performance evaluation in FEMA P-695

In FEMA P-695, the structural models are divided into two performance groups as archetypes with $T \leq T_s$ and $T > T_s$, where T is the fundamental period of the structure and T_s is the transition period (the period between the constant acceleration and constant velocity regions of the design spectrum). Then, both nonlinear static analysis and Incremental Dynamic Analysis (IDA) were performed on the models. The lateral load pattern used in the static nonlinear analysis was proportional to the fundamental mode shape of the archetype model. The 44 far-field ground motion records provided in Table A-4A of FEMA P-695 [22] were utilized for the IDA. The steps in evaluating the performance are as follows [26]:

1. The collapse probability is calculated using Col-

lapse Margin Ratio (CMR) defined as follows:

$$CMR = \frac{\hat{S}_{CT}}{S_{MT}}, \tag{2}$$

where $\hat{S}_{CT}$ is the median collapse capacity obtained from the nonlinear dynamic analysis and S_{MT} is the Maximum Considered Earthquake (MCE) ground motion spectral demand.

2. Adjusted Collapse Margin Ratio (ACMR) is calculated by multiplying CMR and a Spectral Shape Factor (SSF):

$$ACMR_i = SSF_i \times CMR_i. \tag{3}$$

SSF which is a function of the fundamental period (T), period-based ductility ($\mu_T = \delta_u/\delta_{y,eff}$), and applicable Seismic Design Category (SDC) is determined using Table 7-1 of FEMA P-695 [22]. While computing the period-based ductility, δ_u is the ultimate roof displacement defined as the roof displacement corresponding to 0.8 $V_{\max}$, where $V_{\max}$ is the maximum shear force of the fully yielded system and $\delta_{y,eff}$ is the effective yield roof displacement defined as follows:

$$\delta_{y,eff} = C_0 \frac{V_{\max}}{W} \left[\frac{g}{4\pi^2}\right] (\max(T, T_1))^2, \tag{4}$$

where W is the building weight, g is the gravity acceleration, T is the fundamental period of the structural model determined by Eq. 5-5 of FEMA P-695 [22], and T_1 is the fundamental period of the structure calculated via modal analysis. The coefficient C_0 relates the fundamental mode displacement to the roof displacement and can be estimated as:

$$C_0 = \phi_{1,r} \frac{\sum_1^N m_i \phi_{1,i}}{\sum_1^N m_i \phi_{1,i}^2}, \tag{5}$$

where m_i is the mass at the story level, i, $\phi_{l,i}(\phi_{l,r})$ is the ordinate of the fundamental mode at story level i (r represents roof), and N is the number of stories. Figure 2 depicts the maximum base shear force, yield, and ultimate state in FEMA P-695 methodology.

3. The acceptable values of the ACMR of the system are estimated. These values are denoted by $ACMR_{10\%}$ and $ACMR_{20\%}$ for each performance group and individual archetype, respectively. The subscripts 10% and 20% refer to the probability limits of collapse due to MCE ground motions. According to Table 7-3 of FEMA P-695 [22], the values of $ACMR_{10\%}$ and $ACMR_{20\%}$ are determined based on the total system collapse uncertainty (β_{TOT}), which depends on the quality grades related to the design requirements (β_{DR}), nonlinear models (β_{MDL}), test data (β_{TD}), and record-to-record variability (β_{RTR}), as calculated below:

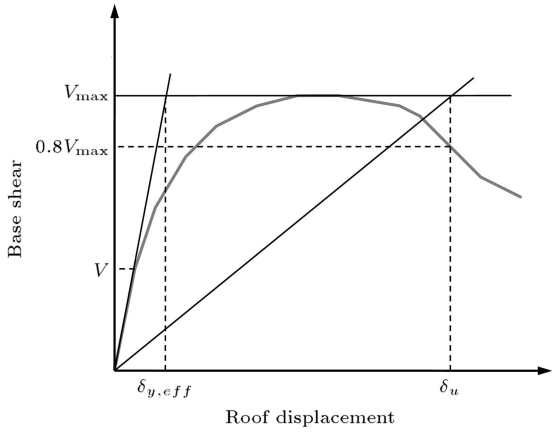

Figure 2. Bilinear idealization of static pushover curve in FEMA P-695 [22].

$$\beta_{TOT} = \sqrt{\beta_{RTR}^2 + \beta_{DR}^2 + \beta_{TD}^2 + \beta_{MDL}^2}, \tag{6}$$

where β_{DR}, β_{TD}, and β_{MDL} are rated as: Superior: $\beta = 0.10$, Good: $\beta = 0.20$, Fair: $\beta = 0.35$, and Poor: $\beta = 0.50$. β_{RTR} is defined as follows:

$$\beta_{RTR} = 0.1 + 0.1\mu_T \leq 0.40. \tag{7}$$

β_{RTR} should be greater than or equal to 0.20. The computed values of ACMR are compared with their acceptable values. Acceptable performance is achieved when the following relationships are satisfied:

$$\overline{ACMR_i} \geq ACMR10\%, \tag{8}$$

$$ACMR_i \geq ACMR20\%, \tag{9}$$

where the subscript i refers to individual archetype and $\overline{ACMR_i}$ is the average value of ACMR for each performance group. In case the system fails to accomplish the required performance objectives, the system should be redefined. Redefining the system could be done by modifying the design requirements, recharacterizing the behavior, and redesigning it using a new trial value of R factor. Then, the new system is reevaluated using the aforementioned methodology.

4. New proposed framework for determining the SPFs

In case the FEMA P-695 methodology is used to evaluate the seismic performance of the diagrid structures, the following problems may arise:

1. In the process of determining the ductility ratio μ using the SPA, the ultimate displacement is regarded as the roof displacement at the point of 20% of the maximum strength loss ($0.8\,V_{\max}$). Since the brittle fracture is the most common failure mode in a diagrid structure, collapse is likely to occur at a displacement before the point of $0.8\,V_{\max}$; thus, determining the ultimate displacement using an alternative method gains significance;
2. Although FEMA P-695 does not directly provide a method for determining the R factor, it validates the R factor used for design of models. It also employs the SPA method to estimate μ and Ω_0 while the IDA technique is applied for assessing the R factor validity. This procedure is based on the assumption that 100% of the effective seismic mass of the structural system contributes to the fundamental mode of vibration. However, in tall or special structures such as diagrid buildings, the effective modal mass ratios for higher modes are taken into consideration. As a result, the SPFs obtained from the pushover analysis may turn out to be highly inaccurate;
3. FEMA P-965 utilizes a set of 44 records for assessing the collapse and validating the R factor. In case the validity of the R factor used in the archetype design is not confirmed, a new (lower) trial value of the R factor must be re-evaluated. Thus, the assessment process can be time consuming.

Given the discussed issues, the following new framework is proposed to determine the SPFs:

1. The archetype model is analyzed using the SPA method. The static pushover curve is plotted and the points corresponding to V_y, $V_{\max}$ and ultimate displacement (δ_u) are determined;
2. The limited numbers of ground motion records (at least 7 records), adequately matched with the design spectrum, are selected from the FEMA P-695 far-field record set to perform the IDA;
3. The IDA is conducted to develop the IDA and Dynamic Pushover Envelope (DPE) curves. To this end, the intensity of ground motion records is gradually increased until the collapse of structural models. The maximum base shear force, roof displacement, inter-story drift, and spectral acceleration are calculated for each earthquake intensity. The IDA and DPE curves are obtained by plotting the spectral acceleration (S_T) versus maximum inter-story drift ratios as well as the maximum base shear force versus the maximum roof displacement, respectively. The method for generating capacity curve (base shear force - roof displacement) is called (DPA);
4. By using the IDA curves, the collapse capacity and ultimate roof displacement for the structural models are determined based on the lateral dynamic instability, as proposed by Vamvatsikos and Cornell [27]. The ultimate roof displacement calculated by the IDA method may exceed the one estimated using SPA method;
5. SPFs are computed using both SPA and DPE curves. The average value for the SPFs calculated by DPA is compared to that for the SPF estimated by SPA, and the higher R factor is selected as a new updated R factor. For a tall or special building, choosing the R factor based on DPA results seems more rational;
6. The structural model is redesigned with the updated R factor and the validity of the modified SPFs is evaluated using the FEMA P-695 procedure. The same ground motion records used for performance assessment are those that have been selected in Stage 3.

The outline of the proposed procedure for determining the SPFs is shown in Figure 3.

5. Designing the structural archetypes and nonlinear models

To evaluate the SPFs and assess the collapse capacity of steel diagrid buildings, a simple square plan with a side of 12 m was selected. All of the lateral and gravity load-resisting members were placed along the perimeter of the buildings. Thus, the buildings have no interior frames. Five archetype models with 6, 8, 10, 12, and 24 stories were designed with a story height of 3.2 m, resulting in height-to-width aspect ratios (H/B) of 1.6, 2.13, 2.67, 3.2, and 6.4 respectively. The diagonal members were placed in 4 m spacing along the perimeter with a fixed slope, approximately 58° regarding the horizontal plane. Figure 4(a)–(d) present the typical configuration of the models used for steel diagrid archetypes. Moreover, box and W sections were used to design the inclined columns and beams, respectively. In diagrid systems, the connections are often prefabricated with considerable fixity, as shown in Figure 5 [28]. To this end, in this study, the beam-column connections are assumed to be moment resisting. The type of steel used in the design process is ASTM A992 with $f_y = 50$ ksi. The dead and live loads of the design were calculated as 6.5 and 2.5 kN/m^2, respectively. To maintain a uniform gravity-load distribution over 4 perimeter frames of the structure, the diaphragm of the floors was considered to be a two-way concrete slab. Seismic design forces and displacements were estimated using the equivalent lateral force method and Response Spectrum Analysis (RSA) as specified in ASCE/SEI 7-10 [29]; in addition, the

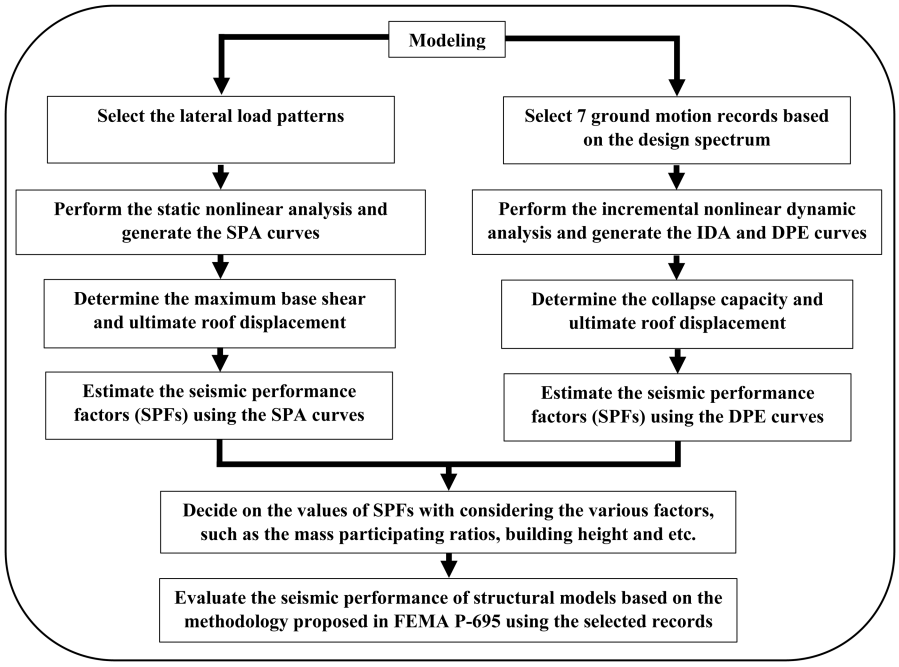

Figure 3. Outline of the proposed procedure for determining the Seismic Performance Factors (SPFs).

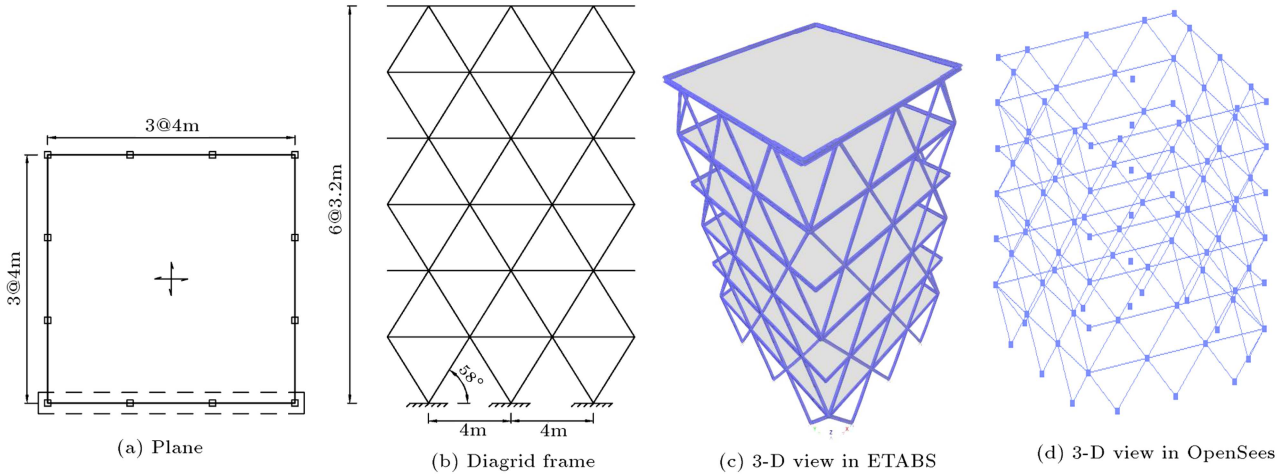

Figure 4. Configuration of the model archetypes.

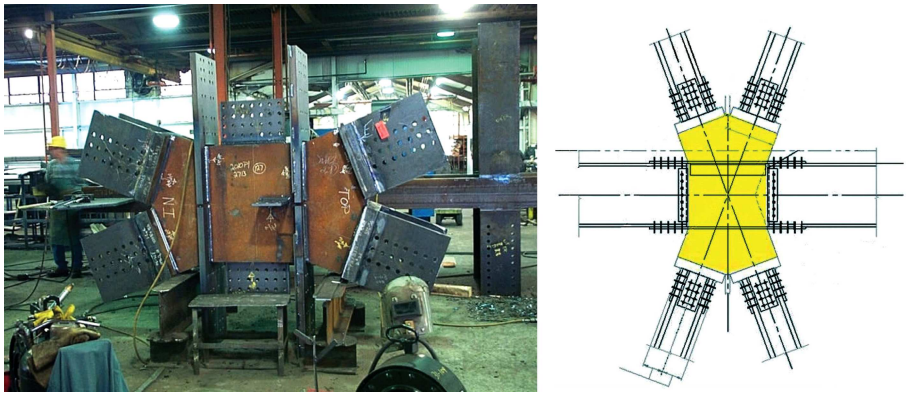

Figure 5. An example of the prefabricated node in the diagrid structure [28].

Load and Resistance Factor Design (LRFD) method in AISC 360-10 [30] was employed in their design. In this study, it was assumed that the diagrid structures were located in a highly seismic zone and the design spectral acceleration parameters were $S_{D1} = 0.6$ g and $S_{DS} = 1$ g. These values are in complete agreement with those for the SDC D_{max} in the FEMA P-695 methodology. To design the models, a building site with soil type D, a seismic importance factor (I_e) of 1.0, and a Rayleigh damping matrix with a damping ratio of 5% for the first two modes were taken into account. Initially, the response modification factor (R factor) was assumed to be 3 and was iteratively updated in the proposed methodology; then, the redesigned structural systems were re-evaluated based on FEMA P-695 methodology. The structural elements were designed using ETABS [31] software, and the OpenSees program was used for nonlinear analyses and collapse evaluation. Table 1 shows the design base shear and dynamic characteristics of the diagrid archetypes.

To prepare the diagrid models in the OpenSees program, each story mass was lumped at the floor level and the floor diaphragm was considered rigid. A nonlinear fiber beam-column element with a section considering the distributed plasticity was utilized for modeling different members. The Menegotto-Pinto material model [32] with isotropic strain hardening of 2% was employed to simulate the mechanical properties of the steel material. In this study, an approach suggested by Uriz et al. [33] was used for modeling the inelastic buckling behavior of the diagonal members. A co-rotational formulation was utilized to model the inclined columns and examine the effects of buckling and large deformation. Figure 6 indicates the model used for the global buckling of diagonal columns. As Uriz et al. [33] suggested in their study, the initial camber of the diagonal columns was 0.1% and the inelastic responses in the critical sections of the elements were estimated by considering 10 to 15 fibers across the depth of the cross-section and 5 integration points along each element. The Newton-Raphson algorithm was used for conducting the nonlinear dynamic analyses. To define the Rayleigh damping matrix, as already explained, the damping ratios for the first two modes were measured as 5%. The initial stiffness matrix of the model was utilized to generate the Rayleigh damping matrices.

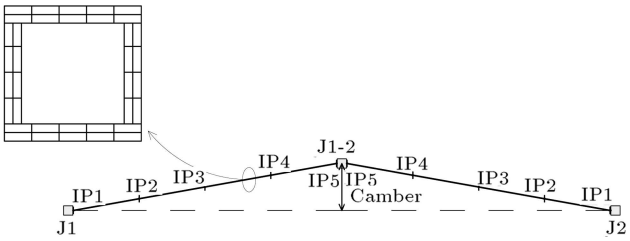

Figure 6. Implemented model to consider the buckling behavior of diagonal members.

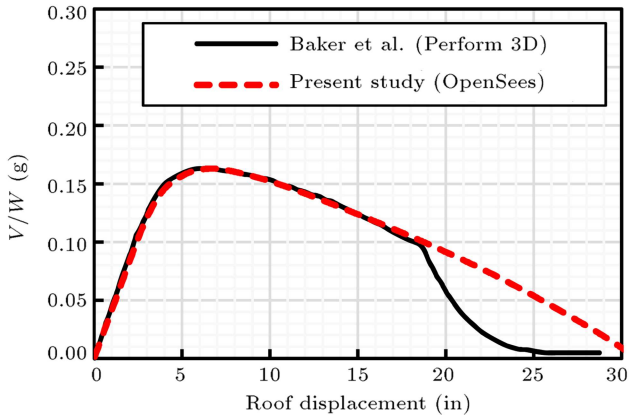

Figure 7. Comparison between the pushover results in OpenSees and findings of Baker et al. [9].

In order to verify the modeling process and the results obtained from the nonlinear analysis, the diagrid structural model used in a recent study conducted by Baker et al. [9] was re-modeled by utilizing OpenSees program and keeping the critical assumptions identical to the original model in Baker's paper. In this model, the post-buckling behavior of the diagonal members in compression is ignored, while the $P - \Delta$ effects are considered in the analysis. Figure 7 compares the results of the NSA of the model prepared in OpenSees program with those obtained by Baker et al. using the Perform-3D program. As observed, the results were in good agreement. The deviation of Baker's results

Table 1. Design base shear force and the modal properties of diagrid models.

Model ID number	V_d (kN)	V_d/W	Fundamental mode	
			Period (sec)	Modal participation mass (%)
6St-Diagrid	1913.6	0.333	0.435	71.5
8St-Diagrid	2565.6	0.333	0.595	67.7
10St-Diagrid	2595.2	0.242	0.826	65.3
12St-Diagrid	2467.6	0.190	1.080	64.2
24St-Diagrid	2683.5	0.113	3.098	59.8

for roof displacements larger than 18 inches seems to be related to the convergence issues of the utilized program.

6. Nonlinear analyses and derivation of R factor

The gravity loads for nonlinear analyses are given in the following load combination:

$$1.05D + 0.25L, \tag{10}$$

where D and L are dead and live loads, respectively. To perform the nonlinear SPA, a lateral load pattern corresponding to the fundamental mode shape and mass distribution of the structure was applied, as shown in the following:

$$F_x \propto \ \mathrm{m_x}\Phi_{1,\mathrm{x}}, \tag{11}$$

where F_x, m_x, and $\phi_{1,x}$ are the story seismic force, story mass, and ordinate of the fundamental mode at level x, respectively. To perform the IDAs, seven earthquake records with adequate agreement with the design spectrum were selected from FEMA P-695 far-field record set. Table 2 shows the characteristics of the selected ground motion records. Figure 8 depicts the response and design spectra of the selected records.

Figure 9(a)–(e) show the static and dynamic pushover curves of the diagrid structural models. The points corresponding to the design base shear, yield, and ultimate displacement are marked on the pushover curves. As shown in these figures, the DPE curves of the 24-story archetype have larger dispersion than other mid-rise model buildings, indicating the sensitivity of the nonlinear structural response of tall diagrid buildings to the time-varying frequency content of ground motion records. Furthermore, the values for SPFs of the proposed models are provided in Table 3. Given the SPFs data obtained from DPE curves, the curves for the probability of exceedance are generated employing a cumulative distribution function defined by Eq. (12):

$$F(SPF = X) = 1 - \Phi\left(\frac{X - \mu}{\sigma}\right), \tag{12}$$

where F is the probability of exceedance corresponding to the SPF equal to X, Φ is the normal cumulative distribution function, and μ and σ are the mean and standard deviation of the SPF values, respectively. Figure 10 shows the exceedance probability curves for SPFs of the diagrid models. For mid-rise buildings with 6–12 stories, the average values of R calculated by SPA and DPA methods are 3.45 and 3.81, respectively. Although the R factor calculated by the SPA method is slightly conservative, the results of these two methods are consistent for mid-rise diagrid buildings. For tall 24-story buildings, the value of R factor calculated by the SPA method is significantly different from that computed using the DPA method mainly due to the effect of the higher modes, which is considerable in taller diagrids. This difference is mainly due to the changes in the over-strength factors rather than the ductility factors calculated using these two methods. Furthermore, the standard deviation of the R values calculated by DPA method is quite larger for 24-story diagrids than other archetypes, easily observed in the exceedance probability curves for R factors.

The obtained results clearly show the need for more comprehensive studies before making a rational decision regarding the R factor of this archetype model. In this regard, by considering the importance of the utilized load pattern in the SPA approach, the effects

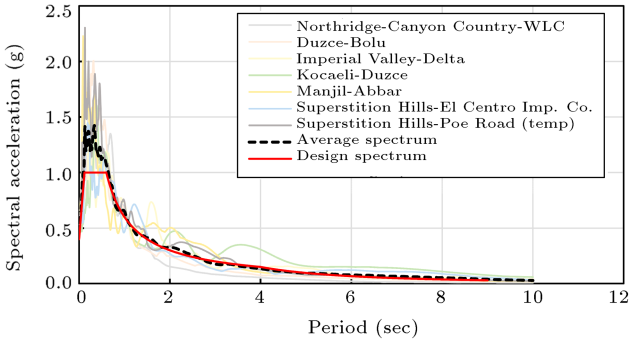

Figure 8. The design spectrum and the response spectra of the selected records.

Table 2. Earthquake record information.

EQ ID	M	Year	Earthquake name	Recording station	PGA (g)	PGV (cm/s)
1	6.7	1994	Northridge	Canyon Country-WLC	0.472	41.128
2	7.1	1999	Duzce, Turkey	Bolu	0.739	55.934
3	6.5	1979	Imperial Valley	Delta	0.35	32.999
4	7.5	1999	Kocaeli, Turkey	Duzce	0.312	58.867
5	7.4	1990	Manjil, Iran	Abbar	0.497	50.591
6	6.5	1987	Superstition Hills	El Centro Imp. Co.	0.357	48.071
7	6.5	1987	Superstition Hills	Poe Road (temp)	0.286	29.016

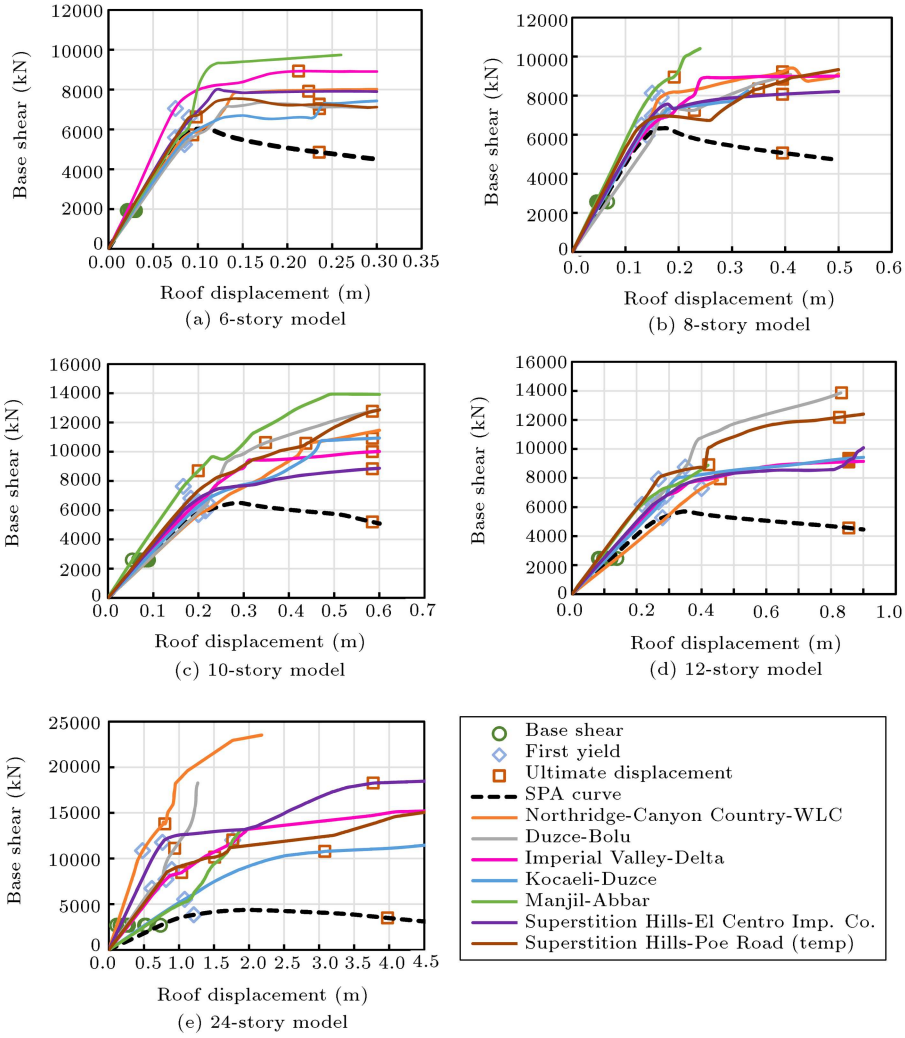

Figure 9. The static and dynamic pushover curves.

Table 3. The computed seismic performance factors for the diagrid models.

Model ID number	SPF	Procedure									
		DPA method									
		EQ ID1	EQ ID2	EQ ID3	EQ ID4	EQ ID5	EQ ID6	EQ ID7	Average	Standard deviation	SPA method
6St-Diagrid	Ω_0	2.82	2.74	3.68	2.85	3.17	2.92	3.45	**3.09**	**0.36**	**2.99**
	R_μ	1.27	1.21	1.34	1.21	1.23	1.34	1.15	**1.25**	**0.07**	**1.28**
	R	3.60	3.32	4.94	3.45	3.91	3.92	3.98	**3.87**	**0.53**	**3.81**
8St-Diagrid	Ω_0	3.05	2.80	2.43	2.74	3.17	2.83	2.56	**2.80**	**0.26**	**2.25**
	R_μ	1.22	1.19	1.45	1.35	1.35	1.35	1.56	**1.35**	**0.13**	**1.58**
	R	3.71	3.34	3.51	3.70	4.28	3.83	4.00	**3.77**	**0.31**	**3.56**
10St-Diagrid	Ω_0	2.20	2.51	2.54	2.48	3.42	2.56	2.71	**2.63**	**0.38**	**2.25**
	R_μ	1.41	1.28	1.41	1.41	1.41	1.54	1.54	**1.43**	**0.09**	**1.46**
	R	3.10	3.22	3.58	3.49	4.82	3.93	4.16	**3.76**	**0.60**	**3.29**
12St-Diagrid	Ω_0	2.93	3.55	2.61	2.74	2.56	2.53	3.23	**2.88**	**0.39**	**2.04**
	R_μ	0.95	1.09	1.43	1.31	1.75	1.52	1.43	**1.35**	**0.27**	**1.54**
	R	2.78	3.85	3.72	3.59	4.48	3.85	4.61	**3.84**	**0.61**	**3.14**
24St-Diagrid	Ω_0	3.64	2.66	2.93	2.12	2.39	4.47	3.21	**3.06**	**0.80**	**1.40**
	R_μ	2.21	1.34	1.28	1.75	1.48	1.70	2.24	**1.71**	**0.39**	**1.84**
	R	8.02	3.57	3.74	3.72	3.53	7.61	7.17	**5.34**	**2.13**	**2.56**

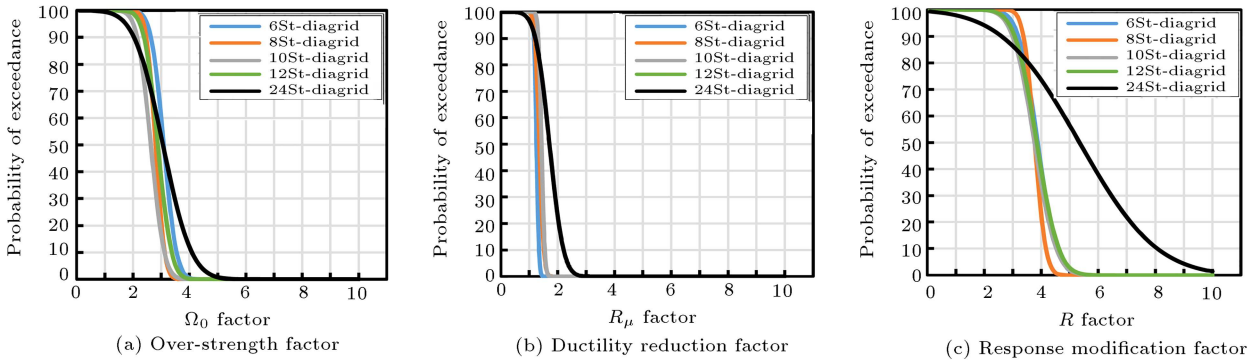

(a) Over-strength factor (b) Ductility reduction factor (c) Response modification factor

Figure 10. The probability of exceedance curves for the seismic performance factors.

of using both other available load patterns in the SPA method and the large number of earthquake records in the DPA method on the SPFs of taller diagrid structures can be examined.

7. Further investigation of *R* factor for the 24-story diagrid model

As discussed earlier, in addition to the lateral load pattern suggested by FEMA P-695 and most of the seismic building codes shown in Eq. (11), the effects of the following lateral load patterns on the results of the SPA are investigated including:

1. Triangular force distribution;
2. Uniform force distribution;
3. Lateral load distribution based on the SRSS combination of the effective modes, as shown in the following [34]:

$$F_i = \sqrt{\sum_{j=1}^{N} (\Gamma_j \phi_{ij} S_{aj} m_i)^2}. \tag{13}$$

4. Lateral load distribution based on the definition of an equivalent fundamental mode $\bar{\phi}_i$, defined as [34]:

$$F_i = \frac{m_i \bar{\phi}_i}{\sum_{k=1}^{N} m_k \bar{\phi}_k}, \tag{14}$$

where $\bar{\phi}_i$ is determined through a combination of effective modes using the SRSS method as follows:

$$\bar{\phi}_i = \sqrt{\sum_{j=1}^{N} (\phi_{ij} \Gamma_j)^2}. \tag{15}$$

5. Lateral load distribution based on the combination of the effective modes according to the Direct Vectorial Addition (DVA) method as described by [35,36]:

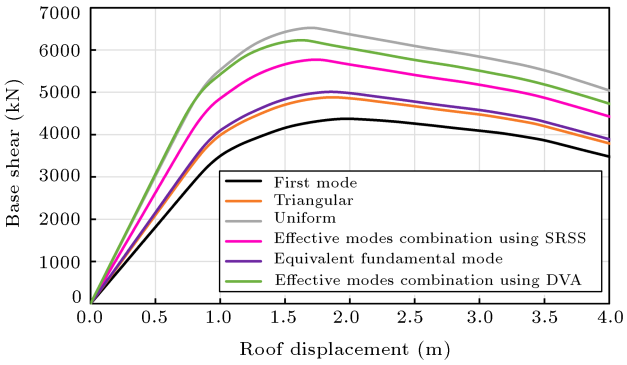

Figure 11. The static pushover curves for the 24-story diagrid model for different load patterns.

$$F_i = \sum_{j=1}^{N} (\eta_j \Gamma_j \phi_{ij} S_{aj} m_i), \tag{16}$$

where F_i and m_i are the story seismic force and story mass of the ith story, respectively; N is the number of the considered modes, ϕ_{ij} is the ith amplitude component of the jth vibration mode; S_{aj} is the pseudo-spectral acceleration of the jth mode; Γ_j is the modal participation factor of the jth mode; and η_j is the modal mass coefficient of the jth mode.

Figure 11 shows the static pushover curves of the model for different load patterns. The values of SPFs estimated by the SPA procedure for different load patterns are summarized in Table 4.

For the types of load patterns (4, 5, and 6), all the modes for which the sum of effective modal masses was more than 90% of the total structural mass could be considered as the effective modes. The maximum R factor of 4.3 was obtained for the load pattern defined by Eq. (16), in which the effect of higher modes was considered, and the minimum R factor of 2.57 was found when the effect of higher modes was neglected (i.e., Eq. (11)). Thus, as expected, the higher modes have considerable effect on the response modification factor of the diagrid archetype.

Table 4. The estimated Seismic Performance Factors (SPFs) by Static Pushover Analysis (SPA) procedure for different load patterns.

Load pattern	Ω_0	R_μ	R
Type (1): First mode	1.40	1.84	2.57
Type (2): Triangular	1.59	1.87	2.97
Type (3): Uniform	2.22	1.92	4.27
Type (4): Combination of effective modes using SRSS	1.95	1.91	3.72
Type (5): Equivalent fundamental mode	1.64	1.87	3.05
Type (6): Combination of effective modes using DVA	2.15	2.01	4.34

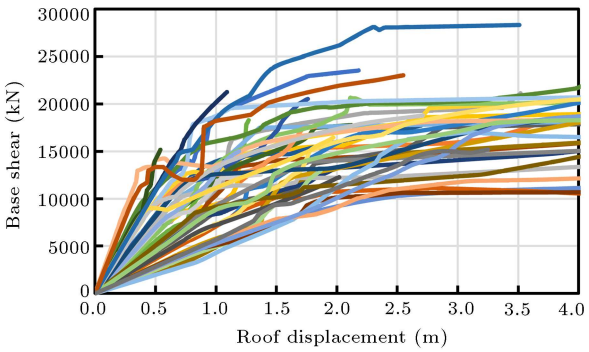

Figure 12. The Dynamic Pushover Envelope (DPE) curves for the 44 earthquake records for the 24-story diagrid model.

To evaluate the effect of using more earthquake records on the outcome of the DPE approach, in addition to the 7 ground motion records considered previously, 37 new records were included. The properties of these ground motions are presented in Tables (A-4A)–(A-4D) of FEMA P-695 [22]. Figure 12 shows the DPE curves of the 44 ground motion records. The values of SPFs are shown in Figure 13. The results exhibit the effects of earthquake frequency content on the response modification factor of the diagrid model. For the 24-story diagrid model, the median value of the R factor calculated by the DPA method is equal to 5.26, while its average value according to the SPA method is 3.49.

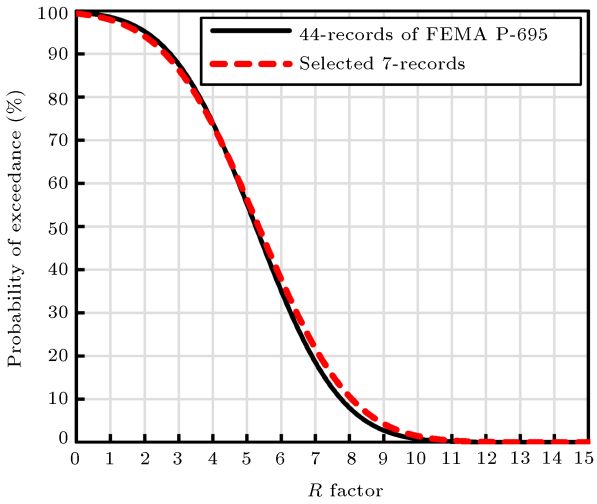

Figure 14. Comparison of the probability of exceedance curves for the R factor.

Therefore, the results obtained by the SPA method are conservative. Given the results determined for the 24-story archetype and other models, considering an R factor equal to 4 can be rational. Figure 14 compares the probability of exceedance curve obtained using the 7 records, selected in Section 6, with the one generated from the 44 earthquake records utilized in this section. It can be seen that the curves are nearly identical.

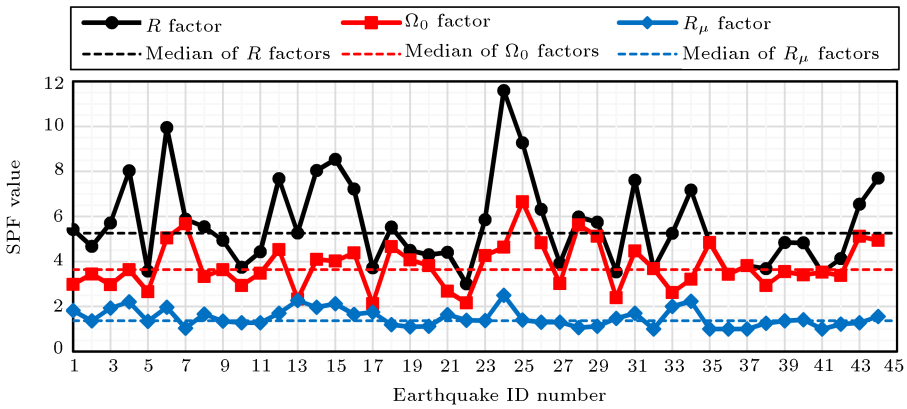

Figure 13. The Seismic Performance Factors (SPFs) calculated by using the Dynamic Pushover Analysis (DPA) method for the 24-story diagrid model.

Table 5. The performance evaluation results for the steel diagrid archetypes.

Model ID number	Procedure	$S_{MT}[T]$ (g)	$\hat{S}_{ct}$ (g)		β_{TOT}	CMR	SSF	ACMR	Acceptance check	
			Value	Error (%)					Acceptable ACMR	Pass/ Fail
Performance group no. diagrid-1 ($T < Ts$)										
6St-Diagrid	FEMA P-695 (44 records)	1.5	3.962	15.71	0.688	2.64	1.190	3.14	1.78	Pass
	New method (7 records)		3.340			2.23		2.65		Pass
8St-Diagrid	FEMA P-695 (44 records)	1.5	3.815	0.17	0.690	2.54	1.211	3.08	1.78	Pass
	New method (7 records)		3.822			2.55		3.09		Pass
Mean of performance group:	**FEMA P-695 (44 records)**							**3.11**	**2.42**	**Pass**
	New method (7 records)							**2.87**		**Pass**
Performance group no. diagrid-2 ($T > T_s$)										
10St-Diagrid	FEMA P-695 (44 records)	1.09	3.240	0.67	0.684	2.97	1.224	3.64	1.77	Pass
	New method (7 records)		3.218			2.95		3.61		Pass
12St-Diagrid	FEMA P-695 (44 records)	0.85	2.222	12.97	0.700	2.60	1.263	3.29	1.80	Pass
	New method (7 records)		2.510			2.94		3.71		Pass
24St-Diagrid	FEMA P-695 (44 records)	0.51	1.008	3.22	0.700	1.99	1.346	2.67	1.80	Pass
	New method (7 records)		1.041			2.05		2.76		Pass
Mean of performance group:	**FEMA P-695 (44 records)**							**3.20**	**2.44**	**Pass**
	New method (7 records)							**3.36**		**Pass**

8. Performance evaluation

By using the IDA technique, the collapse ground motion intensity of archetypes under the effect of each record is obtained based on the dynamic instability criteria. The median collapse acceleration ($\hat{S}_{CT}$) and the CMR are determined using both the 44 records provided in FEMA P-695 and the 7 records selected in the newly proposed method. These values are summarized in Table 5. Using the collapse data extracted from the IDA results, the collapse fragility curve is obtained for each model. The collapse fragility curve, which expresses the probability of collapse as a function of ground motion intensity, is attained by fitting a lognormal cumulative distribution function to the collapse data as follows [37]:

$$P(C/S_T = x) = \Phi\left[\frac{Lnx - \mu}{\beta}\right], \tag{17}$$

where $P(C/S_T = x)$ is the probability of collapse corresponding to a spectral intensity (S_T) equal to x, Φ is the normal cumulative distribution function, and μ and β are the median and standard deviations of $\mathrm{Ln}(S_T)$. Figure 15 compares the collapse fragility curve generated using the 44 records of FEMA P-695 with the one obtained using the selected 7 records. Results confirm the applicability of the proposed methodology for evaluating the seismic performance of diagrid buildings. The seismic performance of diagrid structural models is evaluated based on the methodology proposed in FEMA P-695 by using the 44 ground motion records provided in FEMA P-695 and the 7 ground motion records selected for this study. In that regard, besides the estimation of the ACMR by Eq. (3), the total system collapse uncertainty (β_{TOT}) is also needed. To calculate β_{TOT}, the quality grade for design requirements and index archetype models for the steel diagrid systems is rated good. Moreover, the quality of the test data is considered to be poor because there are not enough test data to assess the seismic capacity of these systems. The values of ACMR and β_{TOT} for diagrid models are summarized in Table 5. The acceptable ACMR is determined based on the total system collapse uncertainty and the acceptable conditional probability of collapse under the MCE ground motions, taken as 10% and 20% for each performance group and each index archetype, respectively.

Performance evaluation results for steel diagrid archetypes are summarized in Table 5 for both the 44 proposed records in FEMA P-695 as well as the selected 7 records in this study. The results show that all diagrid models have sufficient safety against the collapse at the MCE level earthquakes. Therefore, the validity of SPFs is confirmed for the models of diagrid steel structures.

9. Conclusions

This study attempted to propose a new, simpler and reliable methodology for estimating the Seismic Performance Factors (SPFs) of steel diagrid structural systems while applying the framework of FEMA P-695

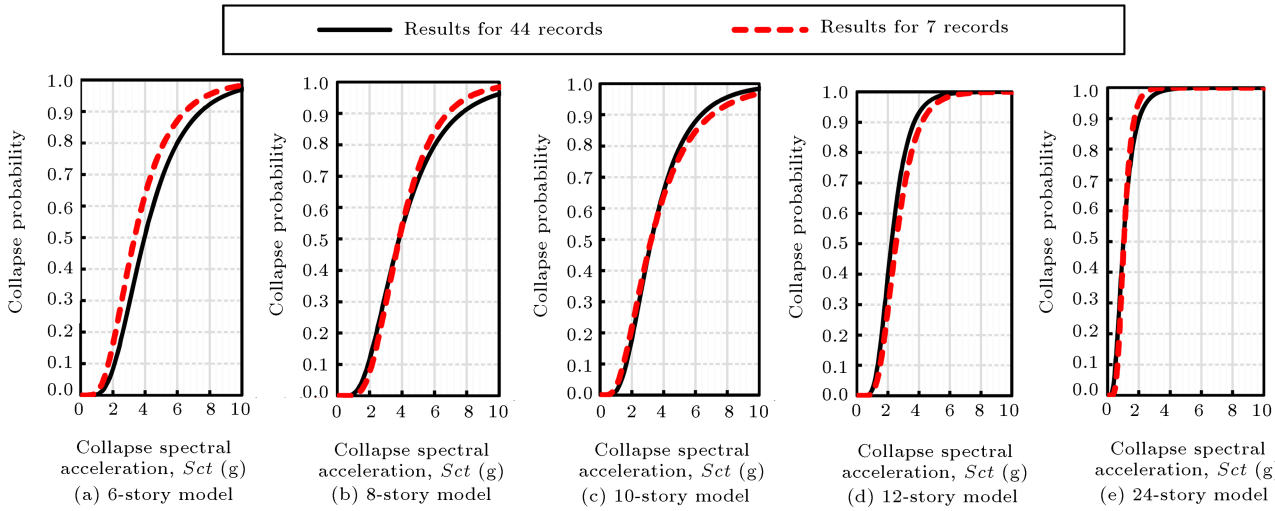

Figure 15. The collapse fragility curves generated using both the 44 records provided in FEMA P-695 and the 7 records selected in the proposed method.

for assessing the validity of SPFs. In the proposed procedure, in addition to the conventional nonlinear static analysis, a probabilistic method based on the Incremental Dynamic Analysis (IDA) technique was also employed for the evaluation of employed SPFs. Also, a limited number of earthquake records would suffice in the final step of seismic performance evaluation in comparison to the 44 ground motion records of FEMA P-695. The results of the current study are summarized in the following:

1. For mid-rise steel diagrid buildings considered in this study, the mean values of over-strength, ductility, and response modification factors obtained from the Static Pushover Analysis (SPA) method were 2.38, 1.46, and 3.45, respectively, while by using the probabilistic method based on the IDA technique, the values of these coefficients became 2.85, 1.34, and 3.81, respectively. In the case of the 24-story tall building with the height-to-width ratio of 6.4, the mean values of over-strength, ductility, and response modification factors calculated by the SPA method for different load patterns were 1.83, 1.90, and 3.49, respectively, while the values of these parameters determined by the probability-based Dynamic Pushover Analysis (DPA) method were 3.64, 1.37, and 5.26, respectively. Therefore, the SPA method obtained a more conservative value for R factor than the probability-based DPA method;
2. The effect of higher modes and frequency content of ground motions on the response modification factor of the tall diagrid model was significant. The use of the first mode load pattern prescribed in FEMA P-695 to perform the SPA yielded unreasonable (over-conservative) R factor values for the 24-story tall archetype, while the lateral load patterns that take into account the effects of higher modes presented results closer to those obtained by the probability-based DPA method;
3. The preliminary results for the diagrid structural system showed that the use of the probability-based DPA method could be suitable for determining the used SPFs. Although the use of more earthquake records could increase the accuracy of results by using this approach, it would prolong the evaluation process. In the proposed framework, a limited number of earthquake records were selected using a method described in the previous sections, and these records were used for the overall assessment of SPFs. For the considered diagrid models, the proposed framework had an acceptable performance in determining the initial R factor. Also, there was an average error of 6.5% in predicting the collapse capacity of diagrids in comparison to the collapse intensity calculated using the FEMA P-695 far-field record set. Although the observed error was relatively low, further studies need to be conducted on the feasibility of using the proposed method for assessing the SPFs of other structural systems. In addition, it is possible to use a limited number of earthquake records in the early stage of evaluation, i.e., for determining the initial R factor and increasing the number of earthquake records in the final stage for assessing the validity of R factor.

References

1. Kim, J. and Lee, Y.H. "Seismic performance evaluation of diagrid system buildings", *The Structural Design of Tall and Special Buildings*, **21**(10), pp. 736–749 (2012).
2. Moon, K.S., Connor, J.J., and Fernandez, J.E. "Di-

agrid structural systems for tall buildings: characteristics and methodology for preliminary design", *The Structural Design of Tall and Special Buildings*, **16**(2), pp. 205–230 (2007).

3. Jani, K. and Patel, P.V. "Analysis and design of diagrid structural system for high rise steel buildings", *Procedia Engineering*, **51**, pp. 92–100 (2013).
4. Montuori, G.M., Mele, E., Brandonisio, G., and Luca, A.D. "Design criteria for diagrid tall buildings: stiffness versus strength", *The Structural Design of Tall and Special Buildings*, **23**(17), pp. 1294–1314 (2014).
5. Milana, G., Olmati, P., Gkoumas, K., and Bontempi, F. "Ultimate capacity of diagrid systems for tall buildings in nominal configuration and damaged state", *Periodica Polytechnica Civil Engineering*, **59**(3), pp. 381–391 (2015).
6. Kamath, K., Hirannaiah, S., and Noronha, J.C.K.B. "An analytical study on performance of a diagrid structure using nonlinear static pushover analysis", *Perspectives in Science*, **8**, pp. 90–92 (2016).
7. Moon, K. "Optimal grid geometry of diagrid structures for tall buildings", *Architectural Science Review*, **51**(3), pp. 239–251 (2008).
8. Zhang, C., Zhao, F., and Liu, Y. "Diagrid tube structures composed of straight diagonals with gradually varying angles", *The Structural Design of Tall and Special Buildings*, **21**(4), pp. 283–295 (2012).
9. Baker, W., Besjak, C., Sarkisian, M., Lee, P., and Doo, C.-S. "Proposed methodology to determine seismic performance factors for steel diagrid framed systems", *CTBUH Technical Paper*, Council of Tall Buildings and Urban Habitat (2010).
10. PERFORM-3D/ Nonlinear Analysis and Performance Assessment for 3D Structures, Computer & Structures Inc., Berkeley, CA (2007).
11. Akbari Hamed, A. and Mofid, M. "Parametric study and computation of seismic performance factors of braced shear panels", *Scientia Iranica, A*, **23**(2), pp. 460–474 (2016).
12. Asghari, A. and Azimi, B. "Evaluation of sensitivity of CBFs for types of bracing and story numbers", *Scientia Iranica, A*, **24**(1), pp. 40–52 (2017).
13. Attia, W.A. and Irheem, M.M.M. "Boundary condition effect on response modification factor of X-braced steel frames", *HBRC Journal*, **14**(1), pp. 104–121 (2018).
14. Etedali, S. and Irandegani, M.A. "A proposed lateral load pattern for pushover analysis of structures subjected to earthquake excitations", *Journal of Vibro-Engineering*, **17**(3), pp. 1363–1371 (2015).
15. Rofooei, F.R. and Mirjalili, M.R. "Dynamic-based pushover analysis for one-way plan asymmetric buildings", *Engineering Structures*, **163**, pp. 332–346 (2018).
16. Liu, Y., Kuang, J.S., and Huang, Q. "Extended spectrum-based pushover analysis for predicting earthquake-induced forces in tall buildings", *Engineering Structures*, **167**, pp. 351–362 (2018).
17. Estekanchi, H.E., Vafai, A., and Basim, M.Ch. "Design and assessment of seismic resilient structures by the endurance time method", *Scientia Iranica, A*, **23**(4), pp. 1648–1657 (2016).
18. Causevic, M. and Mitrovic, S. "Comparison between non-linear dynamic and static seismic analysis of structures according to European and US provisions", *Bulletin of Earthquake Engineering*, **9**(2), pp. 467–489 (2011).
19. Mourad, B. and Sabah, M. "Comparison between static nonlinear and time history analysis using flexibility-based model for an existing structure and effect of taking into account soil using domain reduction method for a single media", *KSCE Journal of Civil Engineering*, **19**(3), pp. 651–663 (2015).
20. Li, S., Zuo, Z., Zhai, C., and Xie, L. "Comparison of static pushover and dynamic analyses using RC building shaking table experiment", *Engineering Structures*, **136**, pp. 430–440 (2017).
21. Endo, Y., Pelà, L., and Roca, P. "Review of different pushover analysis methods applied to masonry buildings and comparison with nonlinear dynamic analysis", *Journal of Earthquake Engineering*, **21**(8), pp. 1234–1255 (2017).
22. FEMA P-695 "Quantification of building seismic performance factors", ATC-63 Report, Federal Emergency Management Agency, Washington, DC (2009).
23. OpenSees "Open system for earthquake engineering simulation", version 2.4.5, Pacific Earthquake Engineering Research Center: University of California, Berkeley, from: http://opensees.berkeley.edu/ (2013).
24. ASCE 41-13, "Seismic evaluation and retrofit of existing buildings", American Society of Civil Engineers, Reston, Virginis (2014).
25. Kim, J. and Choi, H. "Response modification factors of chevron-braced frames", *Engineering Structures*, **27**(2), pp. 285–300 (2005).
26. NEHRP Consultants Joint Venture "Evaluation of the FEMA P-695 methodology for quantification of building seismic performance factors", National Institute of Standards and Technology, U.S. Department of Commerce, Gaithersburg, MD 20899-8600 (2010).
27. Vamvatsikos, D. and Cornell, C.A. "Incremental dynamic analysis", *Earthquake Engineering and Structural Dynamics*, **31**(3), pp. 491–514 (2002).
28. McCain, I. (n.d.) "Diagrid: structural efficiency and increasing popularity", from: http://www.dsg.fgg.uni-lj.si/dubaj2009/images/stories/Diagrid%20tehnologija.pdf, Retrieved October, 15 (2016).
29. ASCE 7-10, *Minimum Design Loads for Buildings and Other Structures*, American Society of Civil Engineers, Reston, VA (2010).

30. AISC 360-10, *Specification for Structural Steel Building*, American Institute of Steel Construction, Chicago, IL (2010).
31. ETABS/ Integrated Building Design Software, Computers and Structures Inc., Berkeley, CA (2013).
32. Menegotto, M. and Pinto, P.E. "Method of analysis for cyclically loaded R.C. plane frames including changes in geometry and non-elastic behavior of elements under combined normal force and bending", *IABSE Symposium on the Resistance and Ultimate Deformability of Structures Acted on by Well Defined Repeated Loads*, Zurich, Switzerland (1973).
33. Uriz, P., Filippou, F.C., and Mahin, S.A. "Model for cyclic inelastic buckling of steel braces", *Journal of Structural Engineering*, **134**(4), pp. 619–628 (2008).
34. Requena, M. and Ayala, G. "Evaluation of a simplified method for the determination of the non-linear seismic response of RC frames", *Proceedings of the Twelfth World Conference on Earthquake Engineering*, Paper 2109, New Zealand Society for Earthquake Engineering, Upper Hutt, New Zealand (2000).
35. Antoniou, S. and Pinho, R. "Advantages and limitations of adaptive and non-adaptive force-based pushover procedures", *Journal of Earthquake Engineering*, **8**(4), pp. 497–522 (2008).
36. Antoniou, S. and Pinho, R. "Development and verification of a displacement-based adaptive pushover procedure", *Journal of Earthquake Engineering*, **8**(5), pp. 643–661 (2008).
37. Ibarra, L.F. and Krawinkler, H. "Global collapse of frame structures under seismic excitations", Technical Report No. 152, John A. Blume Earthquake Engineering Center, Stanford, CA, 324 (2005).

Biographies

Ali Seyedkazemi is currently a PhD candidate in Structural and Earthquake Engineering at Sharif University of Technology, Iran. He is a faculty member at the Civil Engineering Department of Islamic Azad University, Amol, Iran. He received his BSc degree in Civil Engineering from University of Tabriz, Iran in 2003. He received his MSc degree in Structural Engineering from Mazandaran University of Science and Technology, Iran in 2005. His research interests include the structural seismic performance and rehabilitation of existing structures and structures in architecture.

Fayaz Rahimzadeh Rofooei has been a Professor of Civil Engineering at Sharif University of Technology, Iran since 2005. He received his BSc degree in Civil Engineering from Iran University of Science and Technology. He received his MSc degrees in Mathematics and Structural Optimization and also PhD degree in Civil Engineering (Structural Control) from Rensselaer Polytechnic Institute, Troy, N.Y., USA. His research interests are active and passive structural control, nonlinear structural analysis, base isolation, seismic vulnerability analysis, and retrofitting of structures and lifelines.